

# LATERAL FORCE OF MIXING DRUM IN CONCRETE MIXER TRUCK BASED ON EDEM

YuHuan Gao

*Huaiyin Institute of Technology, Huaian 223200, Jiangsu, China.*

*Corresponding Email: 806892554@qq.com*

**Abstract:** Concrete demonstrates fluid properties, which results in specific dynamic behaviors during the transit of concrete mixer trucks. A defining operational trait of these vehicles is that their Concrete Mixing Drum sustain continuous rotation while the trucks are in motion. When a concrete mixer truck makes a turn, the concrete inside the Concrete Mixing Drum undergoes load migration—a phenomenon primarily induced by the combined effects of the concrete's intrinsic fluidity and the centrifugal force generated by the Concrete Mixing Drum's rotation. This load migration is often accompanied by dynamic impacts that exert forces on the Concrete Mixing Drum and the vehicle's chassis. Notably, when the truck's speed increases slightly, the aforementioned load migration and dynamic impacts further deteriorate the vehicle's roll stability. Once the roll stability drops below a critical level, the risk of the truck encountering a rollover accident rises significantly, potentially endangering road safety, property, and human lives. To address this pressing issue, the present study focuses on investigating the Lateral Force generated during the concrete mixing process, as these forces are key factors contributing to the compromised roll stability of the vehicle. To achieve this research goal, EDEM software—a specialized tool for discrete element method simulations—was utilized to conduct numerical simulations of the concrete mixing process inside the Concrete Mixing Drum. The simulations were designed to cover two distinct Filling Ratio conditions of the Concrete Mixing Drum: one with a Filling Ratio of 1:1, corresponding to a total mass of concrete and aggregates of 10,000 kg, and the other with a Filling Ratio of 1:1.2, where the total mass of concrete and aggregates amounts to 12,000 kg. Additionally, three different Rotational Speed of the Concrete Mixing Drum—2 rpm (revolutions per minute), 5 rpm, and 10 rpm—were incorporated into the simulations to examine their respective influences on the generation and magnitude of Lateral Force. By analyzing the simulation data under these varied conditions, the study aims to gain insights into how Filling Ratio and Concrete Mixing Drum Rotational Speed affect Lateral Force characteristics, thereby providing a theoretical foundation for enhancing the roll stability of concrete mixer trucks and mitigating the risk of rollover accidents.

**Keywords:** Concrete mixing drum; Filling ratio; Rotational speed; Lateral force

## 1 INTRODUCTION

Concrete mixer trucks are specialized engineering vehicles in the field of engineering and construction[1]. During the transportation of concrete, the Concrete Mixing Drum of the concrete mixer truck needs to rotate continuously to prevent concrete segregation. Under different Filling Ratio and Rotational Speed conditions, the impact of concrete on the Concrete Mixing Drum may reduce the stability of the concrete mixer truck, making it prone to rollover under the influence of the Concrete Mixing Drum's rotation when turning. In 2016, Sun Yunqi et al. conducted a simulation study using Workbench software to analyze the stress and deformation of the Concrete Mixing Drum of concrete mixer trucks under braking conditions. Bogdan Cazacliu elaborated on the mixing process of the Concrete Mixing Drum in mixer trucks and also explained the working principle of this type of vehicle. In recent years, rollover accidents of concrete mixer trucks have occurred frequently. Many researchers have explored the causes of rollover of concrete mixer trucks, but there is little research on the Lateral Force generated by the Concrete Mixing Drum when mixing concrete with different Filling Ratio and under different Rotational Speed conditions[2][3]. The concrete carried by concrete mixer trucks has a large mass; the most commonly used 12-cubic-meter concrete mixer truck can carry up to nearly 30 tons of concrete and aggregates. During the rotation of the Concrete Mixing Drum, a huge Lateral Force will be generated, which will have a significant impact on the stability of the concrete mixer truck.

In conclusion, studying the Lateral Force generated by the Concrete Mixing Drum during the mixing process is of positive significance for preventing the rollover of concrete mixer trucks. In this paper, the working conditions close to the actual concrete transportation scenario were selected, including the Concrete Mixing Drum loaded with 10,000 kg and 12,000 kg of concrete and aggregates (with Filling Ratio of 1:1 and 1:2 respectively), as well as the working conditions with Rotational Speed of 2 rpm, 5 rpm and 10 rpm[4].

## 2 SIMULATION DESCRIPTION

### 2.1 Structure of the Concrete Mixing Drum

As the core component of concrete mixer trucks, the 12-cubic-meter mixing drum typically adopts a pear-shaped three-section cylinder structure. Inside the Concrete Mixing Drum, there are double logarithmic spiral blades (with a staggered angle of  $1120^\circ$ ), which feature a segmented variable-parameter design: the maximum angle of the front cone section is  $25^\circ$ , the maximum angle of the cylindrical section is  $20^\circ$ , and the maximum angle of the rear cone section is  $112^\circ$ [5]. This structural design enables the mixing, lifting, and turning of concrete through the spiral pushing effect during rotation, ensuring uniform mixing of materials. Its overall dimensions must match the mixing capacity. meanwhile, the agitating Rotational Speed must comply with relevant standards (e.g.,  $\leq 10$  r/min) to guarantee mixing effectiveness while preventing concrete segregation. The geometric accuracy of the drum wall and blades directly affects the movement trajectory of granular materials and the accuracy of simulation results. Therefore, attention must be paid to the geometric accuracy of the drum wall and blades when modeling the Concrete Mixing Drum. The structural dimension diagram of the Concrete Mixing Drum system is shown in Figure 1.

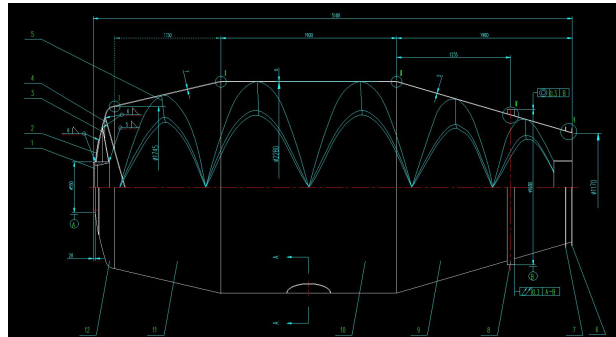


**Figure 1** Structural Dimensions of the Concrete Mixing Drum System

## 2.2 Modeling of the Concrete Mixing Drum

When drawing a 12-cubic-meter Concrete Mixing Drum in SolidWorks, the most critical step is to draw the spiral blades on the corresponding reference plane, rotate them by  $180^\circ$ , and generate a single blade using the "Sweep" function. After completing the modeling of the Concrete Mixing Drum, the model is saved in STL format to facilitate its subsequent import into EDEM software. It is crucial to ensure that an appropriate precision is selected when saving the model in STL format (to avoid excessively high precision leading to an overly large file that impairs simulation efficiency, or excessively low precision resulting in the loss of key structural details such as spiral blades). Meanwhile, check the integrity and geometric accuracy of the spiral blades inside the Concrete Mixing Drum (to prevent deviations in particle motion simulation in EDEM caused by issues such as missing blades or damaged surface areas), and confirm that the model coordinate system is consistent with the EDEM simulation scenario coordinate system. This will reduce the adjustment workload during subsequent scenario construction and ensure the accuracy of the simulation results. The parameters of the concrete mixing drum are shown in Table 1. The view is shown in Figure 2-5.

**Table 1** Parameters of the Concrete Mixing Drum

Name	Total Weight
Nut M8	0.96
Bolt M8×25	1.32
Washer M8	0.048
Liner Plate	2.4
Access Hole Cover Plate	8
Sealing Ring	0.14
Head (or End Closure)	111.65
Front Cylinder Body	418.3
Middle Cylinder Body	639
Rear Cylinder Body	395.9
Concrete Mixing Drum	173.2
Rear Retaining Ring	3.05
Front Retaining Ring	4.06
Spiral Blade Group	282.6
Material Return Plate	101

Inner Support Plate	24.8
Outer Reinforcement Plate	23.3
Flange	57.8

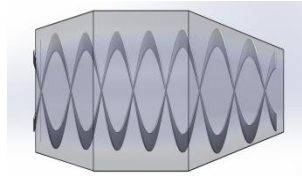


Figure 2 Left View

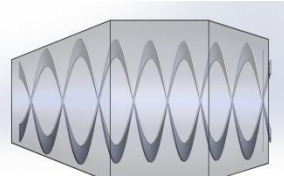


Figure 3 Right View

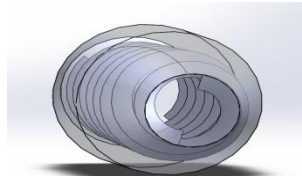


Figure 4 Rear View

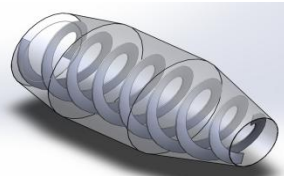


Figure 5 Isometric View

### 2.3 Simulation Scheme

EDEM is a high-performance CAE software based on the Discrete Element Method (DEM), which mainly consists of three components: the pre-processing module, the solver, and the post-processing module. EDEM is equipped with an extensive library of pre-calibrated material models, which allows for quick and easy initiation of simulations and can represent a variety of materials such as rocks, ores, soils, and powders. It features fast and scalable computational performance on CPU, GPU, and multi-GPU solvers, enabling the simulation of large and complex particle systems containing millions or tens of millions of particles. Additionally, custom physical settings can be implemented via EDEM's API for complex simulations and advanced material behaviors, including wet coating, agglomeration, breakage, and magnetic particles.

In the pre-processing module, it is necessary to convert the Concrete Mixing Drum model drawn in Section 2.1 into STL format for import, and establish the coordinate system and global units[6]. In EDEM, particle models can be imported from external sources, and the built-in particle factory can also be used to quickly and easily create corresponding solid particles.[6] Since concrete is a fluid-like material composed of cementitious materials, aggregates, cement, and admixtures, two models—Hertz-Mindlin (no slip) and Hertz-Mindlin with JKR (high cohesiveness)—need to be used in particle modeling to represent concrete particles and aggregates respectively[7]. The JKR model can accurately simulate the bonding between cement paste and aggregates, avoiding the distorted result of "excessive particle dispersion" caused by neglecting cohesion. This enables more reliable optimization of process parameters such as Concrete Mixing Drum rotational speed and pumping pressure, thereby reducing the cost of experimental trial and error[7]. The contact parameters are shown in Tables 2-3. The concrete particle properties are shown in Figure 6.

**Table 2** Settings of Material Properties and Contact Parameters

Material	Density /( $\text{kg}\cdot\text{m}^{-3}$ )	Shear Modulus /( $10^9\text{Pa}$ )	Poisson's Ratio
Aggregate	1450	20	0.35
Cement	1400	70	0.3
Steel	7850	29	0.25

**Table 3** Contact Parameter Settings

Contact Pair	Coefficient of	Coefficient of Static	Coefficient of Kinetic
Steel-Steel Contact	0.2	0.01	0.700
Aggregate- Aggregate Contact	0.7	0.30	0.200
Cement-Cement Contact	0.7	0.20	0.010

Steel-Aggregate Contact	0.6	0.10	0.030
Steel-Cement Contact	0.5	0.35	0.025
Aggregate- Cement Contact	0.8	0.35	0.015

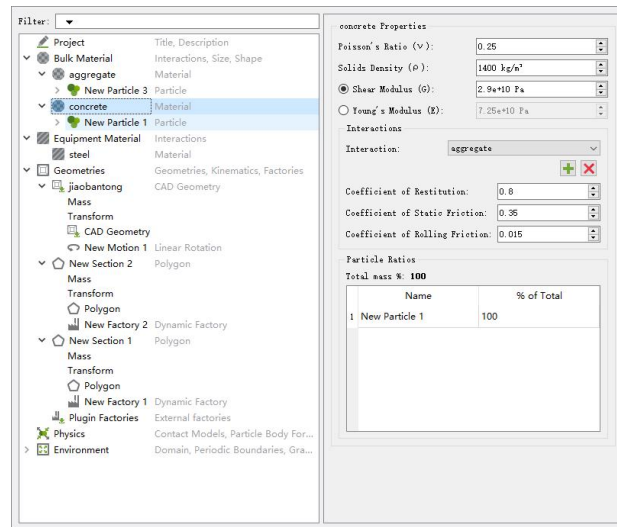


**Figure 6** Concrete Particle Properties

To Facilitate Calculation, the radius of cement particles is set to 0.01 meters, as shown in Figure 7.

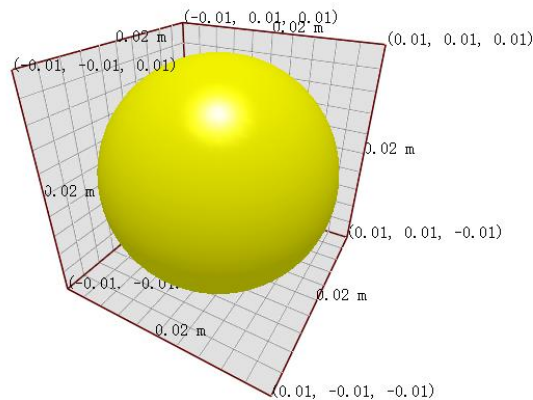


**Figure 7** Properties of Cement Particles

Since concrete exhibits fluid-like behavior, it is necessary to additionally set the properties of two models—Hertz-Mindlin (no slip) and Hertz-Mindlin with JKR (high cohesiveness)—when configuring particles, as shown in Figure 8.

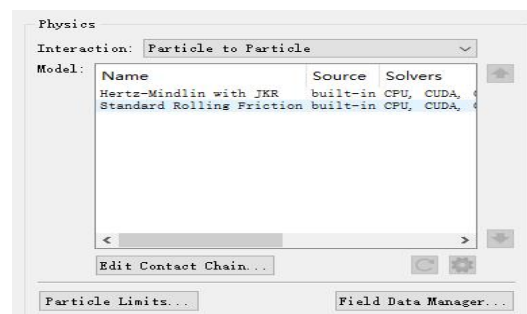


**Figure 8** JKR Model

As a key component of concrete, aggregates typically account for three-fourths of the concrete volume and exert a significant impact on concrete strength; common coarse aggregates include pebbles and crushed stones, while common fine aggregates include natural sand and manufactured sand[8]. During the particle modeling of aggregates, establishing multi-morphology aggregates would incur enormous computational costs in subsequent steps, so to facilitate calculation, the aggregate particle model in this paper is simply set as a single spherical model with a radius of 0.07 meters, and the aggregate properties are shown in Figure 9. From the perspective of concrete performance, the interface bonding state between aggregates and cement paste during the mixing process is one of the core factors determining concrete strength. If mixing is insufficient, the aggregate surfaces will not be uniformly coated with cement paste, leading to the formation of weak interface zones and a subsequent decrease in the compressive and tensile strengths of concrete[9]. Conversely, sufficient mixing enables tight bonding between aggregates and cement paste, which fully exerts the "skeletal support" effect of aggregates and enhances the mechanical properties of concrete. In addition, the water absorption of aggregates also affects the workability of concrete during the mixing process: aggregates with high water absorption (such as natural sand) will absorb water from the cement paste during mixing. If the water dosage is not adjusted in advance, it will easily cause a decrease in concrete slump, thereby affecting the simulation results.

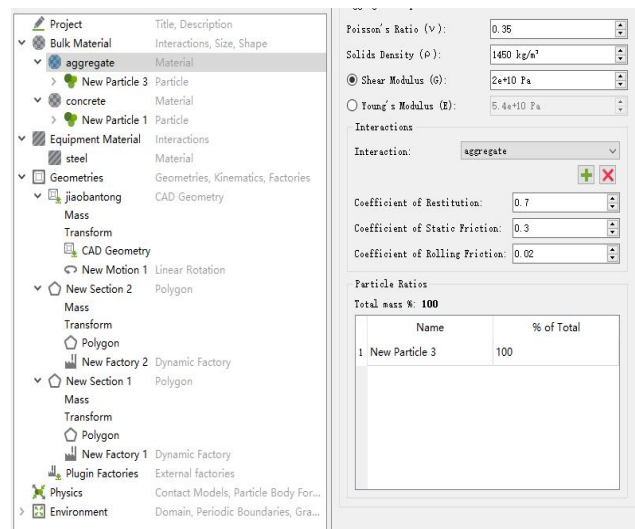


Figure 9 Aggregate Particle Properties

The particle model of aggregates is shown in Figure 10.

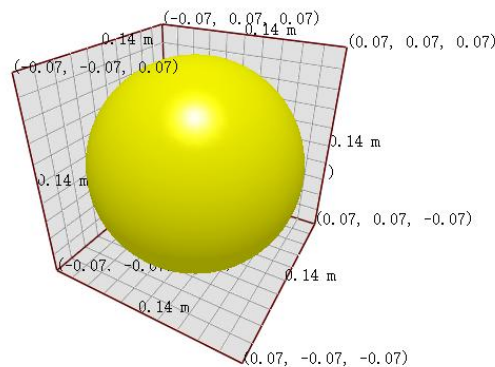


Figure 10 Aggregate Particle Model

## 2.4 Hertz-Mindlin with JKR Contact Model

The Hertz-Mindlin with JKR contact model is a complex yet accurate model in EDEM, mainly used to account for contact scenarios involving surface energy and adhesive effects. Since concrete exhibits fluid-like behavior, the JKR model can better simulate real concrete for simulation purposes. The normal contact force of this model consists of three components: Hertz elastic force, JKR adhesive force, and normal damping force[10]. The relationship is as follows.

$$F_n = F_n^H + F_n^{JKR} + F_n^d \quad (1)$$

$$F_n^H = \frac{4}{3} E^* \sqrt{R^*} \delta_n^{3/2} \quad (2)$$

In Equation (2),  $F_n^H$  denotes the normal contact force,  $E^*$  represents the equivalent elastic modulus, and  $R^*$  stands for the equivalent contact radius[11]. For two spherical particles, the relationship between  $R^*$  and  $R$  (particle radius) is as follows.

$$\frac{1}{R^*} = \frac{1}{R_1} + \frac{1}{R_2} \quad (3)$$

Among them,  $R_1$  and  $R_2$  are the radii of the two particles. When the surface energy is 0, the normal force in Equation (2) becomes the Hertz normal contact force[12].

$$F_{\text{Hertz}} = \frac{4}{3} E^* \sqrt{R^*} \delta^{\frac{3}{2}} \quad (4)$$

In the JKR model, an attractive cohesive force can be provided even when there is no direct contact between two particles. This force is calculated using Equations (5) and (6).

$$\delta_c = \frac{\alpha_c^2}{R^*} - \sqrt{\frac{4\pi\gamma\alpha_c}{E^*}} \quad (5)$$

$$\alpha_c = \left[ \frac{9\pi\gamma R^{*2}}{2E^*} \left( \frac{3}{4} - \frac{1}{\sqrt{2}} \right) \right]^{\frac{1}{3}} \quad (6)$$

When the gap between particles is large or there is no contact, the normal force is zero, while a maximum cohesive force exists. Its expression is as follows.

$$F_{\text{pullout}} = -\frac{3}{2} \pi\gamma R^* \quad (7)$$

In Equation (7),  $F_{\text{pullout}}$  represents the pullout force. The incorporation of the JKR model implies an increase in the computational complexity of the model, which results in significant performance consumption of the computer during large-scale model simulations[13].

## 2.5 Particle Factory

The core function of the EDEM Particle Factory is to quickly and accurately generate qualified particles for discrete element simulations, serving as a key tool for constructing simulation geometries and material models. In this paper, the Particle Factory was used to generate 10,000 kg and 12,000 kg of concrete, as well as concrete-aggregate mixtures with ratios of 1:1 and 1:2. Among them, Factory 1 is responsible for generating concrete particles, while Factory 2 is dedicated to producing aggregate particles, with both generating 200 kg of their respective materials per second. During the initial filling stage of the Concrete Mixing Drum, the Particle Factory was set to "dense packing mode" to optimize particle arrangement density through algorithms, simulating the natural compaction process of concrete under its own weight[14].

This process directly affects the initial contact stress distribution between particles and the drum wall, thereby altering the peak Lateral Force at the moment of mixing startup. The method adopted in this paper is to generate all particles first before rotating the Concrete Mixing Drum, which can avoid the impact of concrete on the peak Lateral Force at the startup moment. When generating particles using the Particle Factory in EDEM, it is essential to focus on multiple key factors to ensure the accuracy and computational efficiency of the simulation: The parameter configuration of particle physical properties should be defined based on specific simulation scenarios, covering key indicators such as density, elastic modulus, and Poisson's ratio that match the characteristics of actual materials, so as to ensure that the particle properties are highly consistent with those of real materials. The particle generation parameters need to be scientifically set: the generation rate should be adapted to the filling sequence of equipment such as the Concrete Mixing Drum to avoid abnormal particle



accumulation caused by excessively high rates or prolonged simulation cycles due to excessively low rates; the particle size and its distribution must strictly conform to the gradation characteristics of actual materials; if a single spherical model is adopted, verification is required to ensure that the particle size selection balances computational accuracy and solution efficiency.

The settings of the Particle Factory are shown in Figures 11-12.

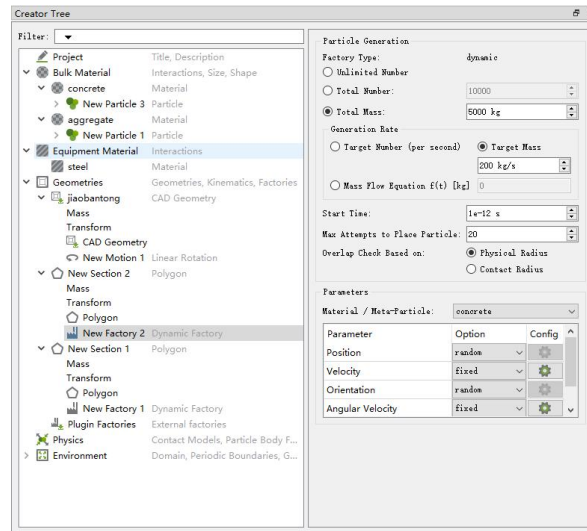


Figure 11 Concrete Particle Factory

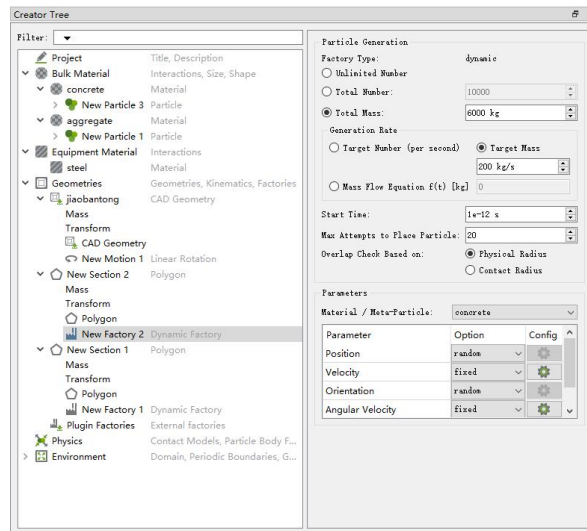
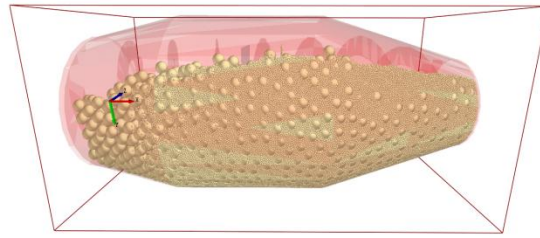


Figure 12 Aggregate Particle Factory

According to the GB/T 26408-2020 standard, the maximum Rotational Speed of the mixing drum of a concrete mixer truck is 18 rpm; the mixing speed during transportation is 1-3 rpm, 6-10 rpm during loading, and 3-14 rpm during unloading. Combined with practical scenarios, the Rotational Speeds of the Concrete Mixing Drum selected in this paper are 2 rpm, 5 rpm, and 10 rpm—among which 10 rpm is used to study the Lateral Force on the concrete mixer drum under extreme transportation conditions. The relationship between Rotational Speed and acceleration is shown in Equation (7) Aggregate Particle Factory

$$\omega = \frac{2\pi n}{60} \quad (8)$$

When the Concrete Mixing Drum rotates at 2 rpm, its angular velocity is approximately 0.209 rad/s when it rotates at 3 rpm, the angular velocity is about 0.524 rad/s and when it rotates at 10 rpm, the angular velocity is roughly 1.047 rad/s. The generated particles are shown in Figure 13.



**Figure 13** Particle Generation Diagram

The radii were set based on the central points at both ends of the Concrete Mixing Drum, and the initial Rotational Speed of the drum was configured. The total time required to generate particles is 30 seconds; to reduce the potential impact of the Concrete Mixing Drum's rotation on the peak Lateral Force during particle generation, the drum was set to start rotating only after 30 seconds. The rotational speed parameters are shown in Figure 14.

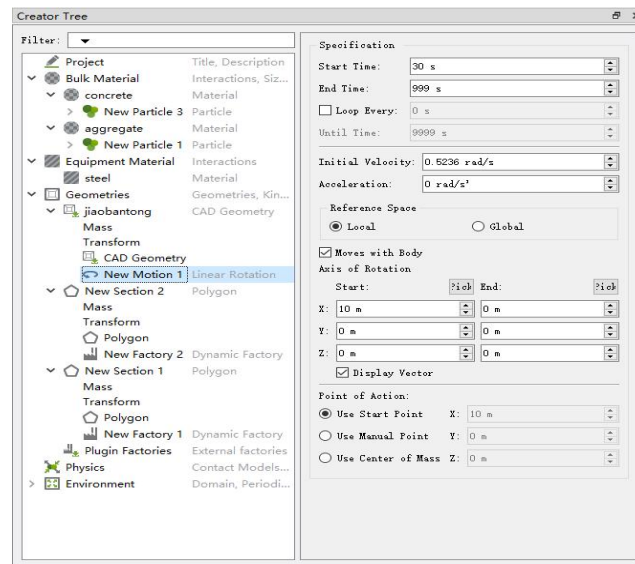


**Figure 14** Rotational Speed Parameters

Since there are no restrictions on the rotation direction, the rotation direction selected in this paper is toward the inside of the screen, as shown in Figure 15.

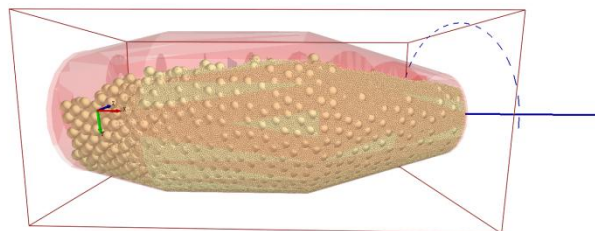


**Figure 15** Rotation of the Concrete Mixing Drum

### 3 PROCESSING OF SIMULATION RESULTS

In the Simulator Settings, the time step was set to 20%, data was saved every 0.1 seconds, and the mesh division size was configured as 2.5R (Cell Size), with a total of 1,820,216 meshes divided. The simulation group parameters and results are shown in Table 4 and Figures 16-20.

**Table 4** Simulation Group Parameters

Time/(s)	Concrete Aggregate Packing Ratio	Weight/(kg)	Rotational Speed/(rpm)
30-35	1:1	10000	10



35-40	1:1	10000	5
40-45	1:2	12000	2
45-50	1:1	12000	5
50-55	1:2	10000	2



Figure 16 30-35 Seconds

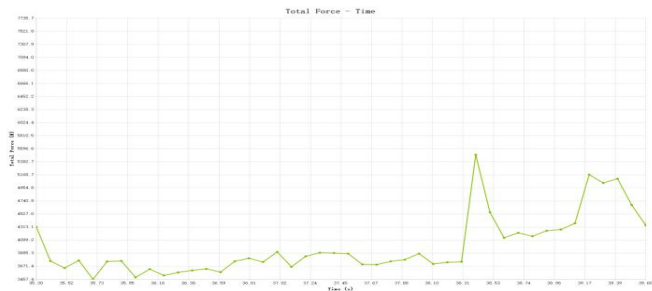


Figure 17 35-40 Seconds



Figure 18 40-45 Seconds



Figure 19 45-50 Seconds



**Figure 20** 50-55 Seconds

#### 4 CONCLUSIONS AND PROSPECTS

From the simulation results, it can be concluded that during the concrete mixing process of the concrete mixer truck, the different packing ratios of concrete and aggregate and the rotational speed of the mixing drum have a significant impact on the lateral force.

1.The simulation results show that when the mass ratio of concrete to aggregate is 1:1 (with a total mass of 10,000 kg) and the rotational speed of the mixing drum is 10 rpm, the peak lateral force exceeds 29,000 N.

2.When the mass ratio of concrete to aggregate is 1:1, the average lateral force is approximately 4,500 N at a rotational speed of 2 rpm; when the rotational speed increases to 5 rpm, the average lateral force can reach 5,500 N. It can be concluded that the faster the rotational speed, the greater the lateral force on the mixing drum, and the greater the threat to the driving safety of the mixer truck.

3.When the rotational speed of the mixing drum is consistently 2 rpm, the peak lateral force in the case of a 1:2 concrete-to-aggregate packing ratio (with a total mass of 10,000 kg) is more than 10,000 N higher than that in the case of a 1:1 packing ratio (with a total mass of 12,000 kg). It can be concluded that the higher the packing ratio, the greater its impact on the lateral force.

4.In this study, the assumed models of concrete spheres and aggregates are ideal spheres. Considering that factors such as the shape and size differences of material particles will affect the simulation results, it may not be possible to obtain highly accurate results. Future research needs to develop more optimization algorithms to improve the accuracy of simulation results.

#### COMPETING INTERESTS

The authors have no relevant financial or non-financial interests to disclose.

#### REFERENCE

- [1] Deng R, Tan Y, Zhang H, et al. Numerical study on the discharging homogeneity of fresh concrete in truck mixer: Effect of motion parameters. *Particulate Science and Technology*, 2018, 36(2): 146-153.
- [2] Yang J, An Q. Mechanics analysis for the main bearing of the rotating drum in the concrete mixing truck. *Journal of the Brazilian Society of Mechanical Sciences and Engineering*, 2018, 40(6): 1-14.
- [3] Fedorko G, Kral J, Kral J, et al. Determination of Calculation for the Shape of Blades Trace in the Concrete Mixer Truck. *Procedia Technology*, 2015, 19, 395-401. DOI: <https://doi.org/10.1016/j.protcy.2015.02.056>.
- [4] Peng J, Shen H, Ding W, et al. Research and analysis of conveyor separation mechanism of light and simple sweet potato combine harvester based on EDEM discrete element method. *Computational Particle Mechanics*, 2025, 1-18. DOI: 10.1007/S40571-025-01031-X.
- [5] Ou M, Wang G, Lu Y, et al. Structure Optimization and Performance Simulation of a Double-Disc Fertilizer Spreader Based on EDEM-CFD. *Agronomy*, 2025, 15(5): 1025-1025.
- [6] Song S, Zhu S, Wang J, et al. Disturbance analysis of shield tunneling in clay and limestone composite strata using EDEM simulation. *Scientific Reports*, 2025, 15(1): 12616-12616.
- [7] Zhao Z, Hou J, Guo P, et al. Analysis of Soil–Straw Movement Behavior in Saline–Alkali Soil Under Dual-Axis Rotary Tillage Based on EDEM. *Agriculture*, 2025, 15(3): 337-337.
- [8] Gong Y, Yu C, Zhang Z, et al. Enhancement of recycled coarse aggregate concrete properties using a combined adjustable cement slurry coating and mixing approach. *Construction and Building Materials*, 2025, 491, 142634-142634.
- [9] Wang X, Zhang Y, Zhang W, et al. Research on improving the performance and mechanism of manufactured sand concrete based on vibration-coupled mixing. *Journal of Building Engineering*, 2025, 108, 112971-112971.

- [10] Jiang D, Soroush M, Yi B, et al. Modeling mixing kinetics for large-scale production of Ultra-High-Performance Concrete: effects of temperature, volume, and mixing method. *Construction and Building Materials*, 2023, 397. DOI: <https://doi.org/10.1016/j.conbuildmat.2023.132439>.
- [11] Guodong C, Lide L, Shiguo L, et al. Numerical flow simulation of fresh concrete in mixing truck. *Powder Technology*, 2022, 409. DOI: <https://doi.org/10.1016/j.powtec.2022.117781>.
- [12] Cristian F, Nicolò B. Mixing Phase Study of a Concrete Truck Mixer via CFD Multiphase Approach. *Journal of Engineering Mechanics*, 2022, 148(3). DOI: [https://doi.org/10.1061/\(ASCE\)EM.1943-7889.0002042](https://doi.org/10.1061/(ASCE)EM.1943-7889.0002042).
- [13] Yuanqiang T, Rong D, Hao Z, et al. Study of mixing and discharging of dry particles in a truck mixer. *Particulate Science and Technology*, 2020, 38(3): 271-285.
- [14] Deng R, Tan Y, Zhang H, et al. Experimental and DEM studies on the transition of axial segregation in a truck mixer. *Powder Technology*, 2016, 314, 148-163.